16th World Congress in Computational Mechanics (WCCM)
21-26 July 2024, Vancouver, Canada
A. Korobenko, M. Laforest, S. Prudhomme, R. Vaziri (Eds)

ENHANCING PREDICTIVE MODELING IN REACTOR BUILDING DOSE DISTRIBUTION: A NEURAL NETWORK-AIDED APPROACH

JIHONG LIU[1], KOJI KOYAMADA[1], HIROAKI NASTUKAWA[1] AND SHUHEI KAMIOKA[1]

[1]Osaka Seikei University
1-3-7, Aikawa, Higashiyodogawa-ku, Osaka, 533-0007, Japan
liu-j@osaka-seikei.ac.jp, https://univ.osaka-seikei.jp/en/

Key words: Radiation dose rate, Surrogate model, Deep learning, Principle of Superposition.

Abstract: *Ensuring the safety of nuclear reactor decommissioning workers requires accurate, real-time predictions of radiation dose rates within reactor buildings. However, due to the complexity of these structures, such predictions are computationally intensive and time-consuming. In this paper, we propose constructing a surrogate model using deep learning to predict radiation dose rates based on simulation results in a space containing a square pillar and a radiation source. The accuracy of the surrogate model's predictions was verified and visualized. Additionally, by applying the principle of superposition, we demonstrated that the distribution of radiation dose rates in spaces with a pillar and multiple radiation sources can be obtained by summing the surrogate model results for each radiation source. We also examined the application of the surrogate model to predicting radiation dose rates in spaces containing multiple square pillars and multiple radiation sources. This approach shows the potential for surrogate models to accurately and efficiently predict radiation dose rates in reactor buildings with complex structures and multiple radiation sources in real time.*

1 INTRODUCTION

In the decommissioning work to address the nuclear reactor damage at the Fukushima Daiichi Nuclear Power Plant (hereinafter referred to as "1F") caused by the Great East Japan Earthquake of 2011, reducing worker exposure and ensuring safety are top priorities [1, 2]. Therefore, it is crucial to predict and control radiation sources and dose rates at the work site in real time with high accuracy.

In general, computer simulations based on radiation transport equations [3] are necessary to accurately predict radiation dose rates in work environments and to determine exposure doses in advance. However, simulating radiation dose rates in the 1F reactor buildings, with their complex structures, requires a significant amount of time and computational resources [4].

To improve the safety of the 1F reactor decommissioning, it is desirable to develop a method that can accurately and quickly predict the radiation dose rates in the reactor buildings. To address this challenge, surrogate models are gaining attention because they can perform simulation-like predictions at high speed by learning from the input data and output results of simulations using machine learning. Surrogate models can make predictions quickly as an alternative to simulations and are used to improve design efficiency and conduct exhaustive parameter searches that are difficult to achieve with traditional simulations [5-9]. However, the methods for model construction and the selection of training data often vary on a case-by-case

basis. Specifically, optimal data and algorithms have not been standardized, requiring trial and error in practice [10, 11]. This calls for the accumulation of knowledge and methods for constructing optimal surrogate models for each field of application.

In this study, we attempted to construct a surrogate model using deep learning to quickly predict radiation dose rates, based on the results of simulations in a space containing a square pillar and a radiation source. The accuracy of the surrogate model's predictions was verified and visualized. Additionally, by applying the principle of superposition, we demonstrated that the distribution of radiation dose rates in spaces with a pillar and multiple radiation sources can be obtained by summing the surrogate model results for each radiation source. We also examined the application of the surrogate model to predicting radiation dose rates in spaces containing multiple square pillars and multiple radiation sources. This approach shows the potential for surrogate models to accurately and efficiently predict radiation dose rates in the reactor buildings with complex structures and multiple radiation sources in real time.

2 SIMULATION OF RADIATION DOSE RATE

This chapter briefly describes the Radiation Transport Equation, which forms the basis for radiation dose rate simulations.

2.1 Radiation transport equation

The radiation transport equation [12], given below, is used to predict the distribution of radiation dose rates. This fundamental equation describes how radiation is transported, scattered, and absorbed within a material. It details the distribution of radiation in terms of space, energy, direction, and time.

$$\frac{\partial I}{\partial t} + \Omega \cdot \nabla I + \sum\nolimits_t I = \int \int_0^\infty \sum\nolimits_s I' dE' d\Omega' + S \tag{1}$$

where I, Ω, and S represent the position, direction, energy, and time-dependent radiation intensity; the direction of radiation travel; and the external radiation sources, respectively. $\sum_t$ is the total attenuation coefficient, which represents the probability that the radiation is absorbed or scattered. $\sum_s$ is the scattering coefficient, indicating the probability that the radiation changes from one energy to another. I' is the radiation intensity before scattering, dE' is the energy range before scattering, and $d\Omega'$ is the directional range before scattering.

The equation is extremely complex and almost impossible to solve analytically. Therefore, numerical simulation methods, such as the Monte Carlo method, are used. From the results of the numerical simulations, the radiation intensity I at a particular location is obtained. The radiation dose rate $\dot{D}$ is obtained by integrating the radiation intensity I with respect to energy and direction as follows, where E represents the energy of the radiation.

$$\dot{D} = \int \int_0^\infty \sum\nolimits_s I dE d\Omega \tag{2}$$

The radiation transport equation is a linear equation with respect to the radiation intensity I. Due to this linearity, the radiation dose rate is also linear. In other words, the principle of superposition applies to the radiation dose rate. Thus, for example, if there is a complex geometry or multiple radiation sources, the overall radiation dose rates can be calculated by

summing the results obtained for each geometry or radiation source separately.

2.2 Simulation of radiation dose rates in a space with a square pillar

In this paper, we simulate the radiation dose rates in a space containing a square pillar and a radiation source, considering different positions of both the pillar and the source. Specifically, as shown in Figure 1, one square pillar is assumed, and its position is shifted incrementally across an 8 × 8 floor grid, resulting in 64 different cases. The positions of the square pillar are numbered from 1 to 8 along the X-axis starting from the origin, then from 9 to 16 along the X-axis after shifting in the Y direction. This pattern is repeated until all 64 cases are numbered.

Conversely, the radiation source is placed on 76 square surfaces (63 on the floor and 13 on the pillar), respectively, corresponding to the surfaces adjacent to the floor and pillar. The locations of the sources on the floor surface are numbered from 1 to 63, similar to the pillar positions. When a pillar is moved, the vacated space is assigned a new number corresponding to its new position, and the number of the new location is removed since the pillar now occupies it. On the surface of the pillar, the top surface is numbered 64, and the surfaces facing the -X and X directions are numbered 65 to 67 and 68 to 70 along the Z direction, respectively. Similarly, the surfaces facing the -Y and Y directions are numbered 71 to 73 and 74 to 76 along the Z direction, respectively.

For each square pillar from No. 1 to No. 64, unit sources (Cs-134 and Cs-137) are placed on the 76 square planes on the floor and the surfaces of the pillar. The radiation dose rates at 9 × 9 × 9 grid points in the space above the floor are then obtained through simulations. This results in a dataset of radiation dose rates consisting of 76 × 9 × 9 × 9 rows for each square pillar. In total, 64 datasets are generated. The coordinates of the grid points in the X, Y, and Z directions range from 0 mm to 80 mm, with a grid spacing of 10 mm.

For the simulation, the software 3D-ADRES-Indoor / PHITS [13, 14], which can accurately analyze radiation propagation in indoor space environments, is used.

Figure 2 shows an example of the distribution of radiation dose rates in the space, calculated by the simulation based on the conditions described above. In this example, the radiation dose rates at the 9 × 9 × 9 grid points in the space above the floor are represented by the colors of the points when the square pillar is at position 1 and the radiation source is at position 32. The isosurfaces of the radiation dose rates in the space, based on the grid point values, is also shown in the same figure. It can be seen that the radiation dose rates are high in the vicinity of the source position and decrease rapidly as the distance from the source increases.

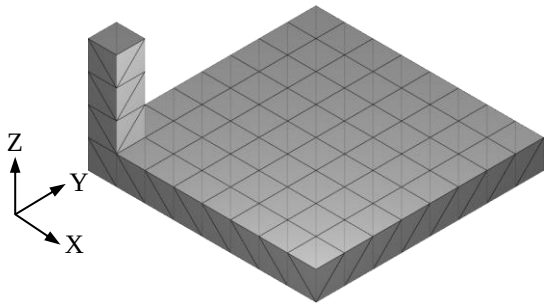

Figure 1: Space with a square pillar.

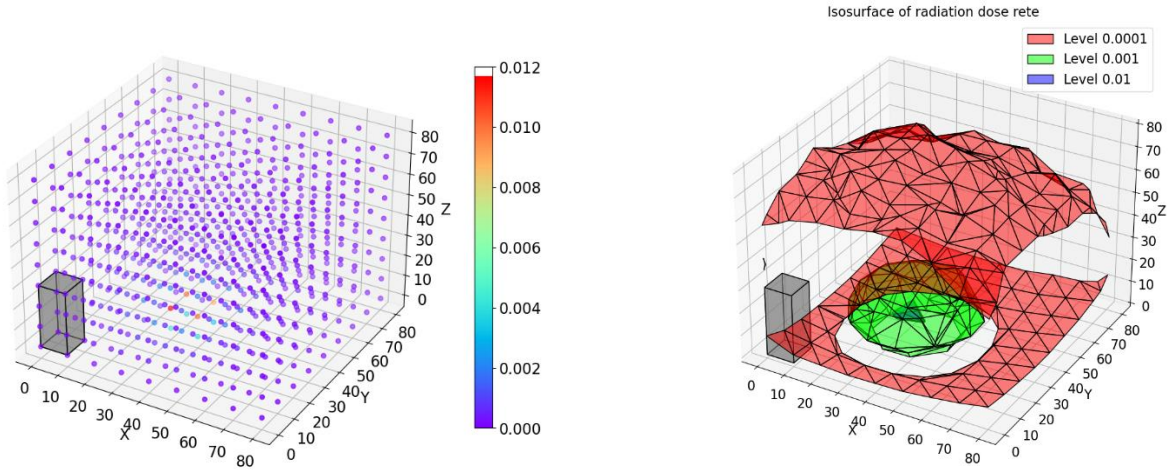

Figure 2: Simulation results of radiation dose rates in a space with a square pillar and a radiation source.

3 CONSTRUCTION OF SURROGATE MODEL

In this chapter, we construct and verify the accuracy of a surrogate model that predicts radiation dose rates using deep learning. This model is based on the radiation dose rates at grid points in a space containing a square pillar obtained from the simulations in the previous chapter.

3.1 Surrogate model construction method

This section describes the construction of a surrogate model using deep learning based on a Deep Neural Network (DNN). The procedure is shown in Figure 3, and the details are as follows.
Data loading: Load the input data and output results necessary to construct the model. In this study, we randomly select and read a certain number of datasets from the total of 64 datasets corresponding to each square pillar obtained from the simulations in the previous chapter.

The input data consists of 13 items: *"SC_num"* and *"RS_num"* indicating the locations of the pillar and the radiation source, *"SC_x"* and *"SC_y"* indicating the coordinates of the pillar center, *"RS_x"*, *"RS_y"*, *"RS_z"*, *"RS_nx"*, *"RS_ny"* and *"RS_nz"* indicating the coordinates and normal directions of the square surface center where the radiation source exists, and *"Grid_x"*, *"Grid_y"* and *"Grid_z"* indicating the coordinates of the grid points in the upper floor space. In this paper, the coordinate of the center of the square pillar *"SC_z"* is not considered in the dataset because the height of the pillar is the same in all 64 cases. It is also important to note that *"SC_num"* and *"RS_num"* are used to identify the location of the pillar and the radiation source and are not used to train the model. The output result has only one entry: the dose rate *"Dose_rate"* at the grid point in the space above the floor.
Data normalization and splitting: First, the data are normalized to a range of 0 to 1, making it suitable for training the model. Next, the data are randomly split into training and validation sets. In this paper, the data are divided into training and validation sets in a ratio of 80% to 20%.
DNN definition: Define the structure of a DNN, including the number of layers, the number of neurons in each layer, the regularization method, the activation function, etc. In this paper, the DNN consists of three layers with 64, 32, and 16 neurons in each layer, respectively. No regularization method is used, and the ReLU function is employed as the activation function.
Model creation definition: The model is compiled, and the optimization method, loss function, evaluation index, etc., are set. In this paper, Adam is used as the optimization algorithm, Mean

Squared Error (MSE) is used as the loss function, and the coefficient of determination (R^2) is specified as the model validation index.

Training and monitoring: Specify training and validation data, batch size, number of epochs, and callbacks. During the training process, validation data are used to verify and monitor the model's performance. In this paper, the model is trained with a batch size of 2048 and 500 epochs. Additionally, a callback saves the model at the point when the R^2 for the validation data is highest during training.

Evaluation: We evaluate the performance of the model on the training and validation data. In this paper, we test the accuracy of the model using the MSE and the R^2 for the training and the validation data during the training process. We also evaluate the generalization performance of the model using the R^2 for the remaining dataset not used to construct the model.

Prediction and visualization: The input data are used to predict the results, which are then visualized. In this paper, we predict the radiation dose rates at grid points in the space above the floor surface with a square pillar and a radiation source at arbitrary locations. Based on the values at these grid points, isosurfaces of the radiation dose rate in the space are shown. In the case of an arbitrarily located pillar and radiation sources, the dose rate at each grid point can be obtained by summing the results of the individual predictions based on the principle of superposition. The distribution of the radiation dose rates is visualized by the isosurface in space.

3.2 Creating a surrogate model

Following the procedure presented in the previous section, we create a surrogate model to predict the radiation dose rates in a space containing a square pillar and a radiation source. In this paper, we first create a surrogate model using randomly selected training datasets. Next, we examine whether the surrogate model can predict radiation dose rates accurately and stably. Furthermore, we estimate the number of training datasets required to create a highly accurate and stable surrogate model.

Model training: Five datasets were randomly selected from the 64 datasets and used as training

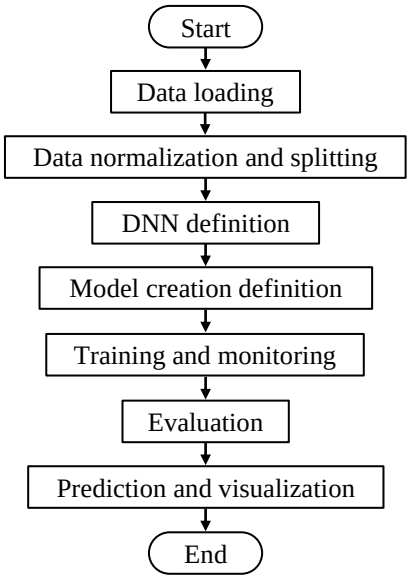

Figure 3: Procedure for constructing a surrogate model by machine learning based on DNN.

datasets to train the model. An example of the change in MSE and R^2 of the training and the validation data as the number of epochs increases during the training process is shown in Figure 4. It can be seen that when the number of epochs reaches approximately 100, the MSE and the R^2 hardly change. For the best performing optimal model, the R^2 for the training and the validation data are close to 1, specifically 0.9976 and 0.9975, respectively, indicating that the optimal model can predict with high accuracy. For additional insight, Figure 4 also presents a 45-degree line plot of the validation data using the optimal model. This figure further demonstrates a good agreement between the surrogate model predictions and the actual simulation results for the radiation dose rates. Taken together, these results confirm the high accuracy of the surrogate model for the five randomly selected datasets.

To evaluate the generalization performance of the surrogate model described above, the R^2 was calculated for each of the remaining 59 datasets that were not used in the model construction (hereafter referred to as the unknown data) by predicting radiation dose rates using the surrogate model. The distribution of the R^2 is shown in the histogram in Figure 5, and the mean, standard deviation (SD), maximum, and minimum values are shown in Table 1. These results confirm that the distribution of the R^2 has small variability. The mean R^2 is 0.9912, which is very close to 1, and the SD is 0.0283, which is sufficiently small to evaluate the generalization performance of the model as good. However, the minimum R^2 is 0.6338, indicating that while the prediction accuracy of the model is generally good overall, there are some cases where the prediction accuracy decreases.

Model stability: In training the above model, it was confirmed that the surrogate model created using five randomly selected datasets from the 64 datasets produced generally good prediction results for the unknown data. However, it is necessary to evaluate whether this result holds true even if different five datasets are selected, i.e., whether the model is stable and can make accurate predictions for the unknown data. In this paper, we evaluate the stability of the model by performing Monte Carlo cross-validation, calculating the R^2 for each trial, and obtaining the mean, SD, maximum, and minimum values.

Figure 6 shows the mean R^2 values and their SDs for the validation and the unknown data after 10, 20, ..., and 100 Monte Carlo cross-validation trials on five randomly selected datasets. Figure 7 shows histograms of the distribution of the R^2 values for the case of 100 trials. These results show that the mean R^2 and the SD become more stable as the number of Monte Carlo

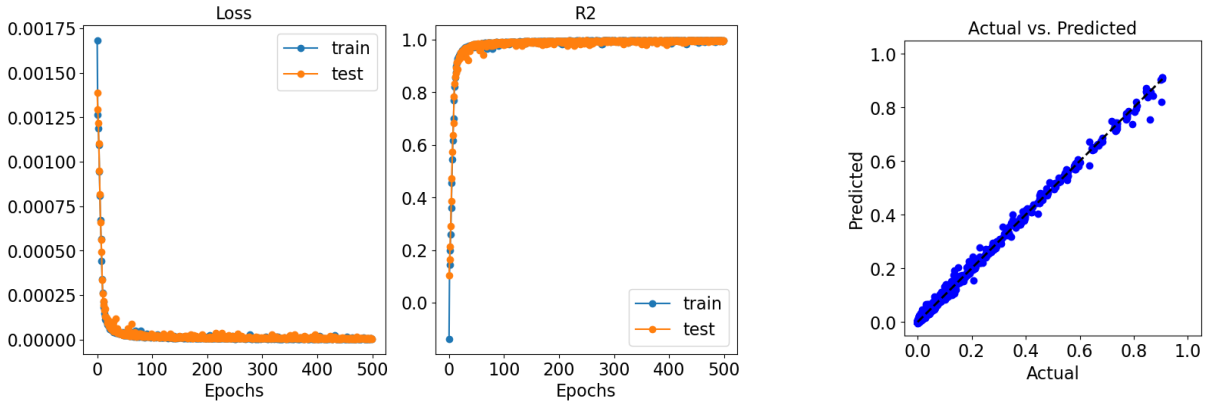

Figure 4: Variation of the loss function and the R^2 with the number of epochs (left), and a 45-degree line plot of the validation data using the optimal surrogate model created from five randomly selected datasets (right).

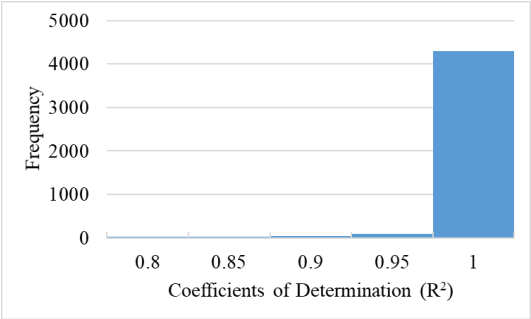

Figure 5: Histogram of the R^2 for the unknown data, generated using the optimal surrogate model created from five randomly selected datasets.

Table 1: Mean, SD, maximum, and minimum R^2 values for the unknown data, which were not used in the surrogate model training.

Mean	SD	Max.	Min.
0.9912	0.0283	0.9997	0.6338

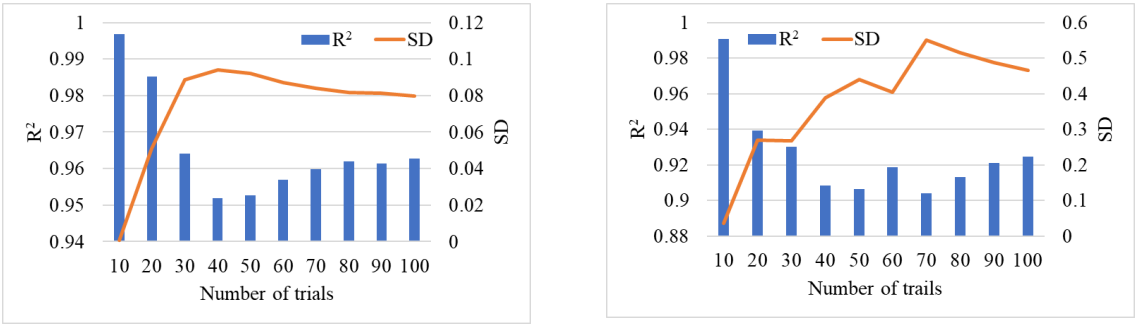

Figure 6: Mean R^2 values and SDs for the validation data (left) and the unknown data (right), obtained through 10, 20, ..., and 100 Monte Carlo cross-validation trials performed on five randomly selected datasets.

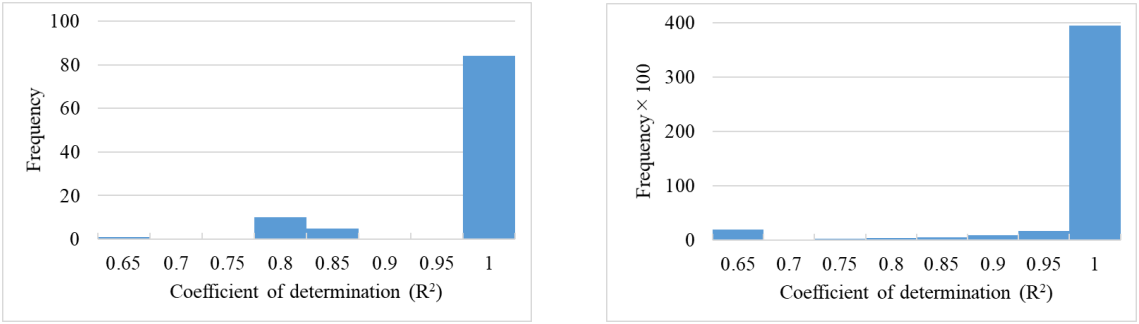

Figure 7: Histogram of the R^2 values for both the validation data (left) and the unknown data (right) for the case of 100 trials, generated using the optimal surrogate model developed from five randomly selected datasets

Table 2: Mean, SD, maximum, and minimum R^2 values for both the validation data and the unknown data based on 100 Monte Carlo cross-validation trails

R^2	Mean	SD	Maximum	Minimum
Test data	0.9628	0.0798	0.9980	0.6290
Unknown data	0.9245	0.4661	0.9997	-18.59

trials increases. It can also be seen from the figure that the mean R^2 values for the validation data are high and their SDs are small, while the mean R^2 values for the unknown data are relatively high, but their SDs are large. Specifically, as shown in Table 2, the mean R^2 values and their SDs for 100 trials are 0.9628 and 0.0798 for the validation data, and 0.9245 and 0.4661 for the unknown data. The maximum R^2 values are 0.9980 for the validation data and 0.9997 for the unknown data, which are all close to 1, indicating very good results. On the other hand, the minimum R^2 is 0.6290 for the validation data, which is generally good, but -18.59 for the unknown data, which is extremely poor. This indicates that when the number of datasets is five, the prediction accuracy may be significantly worse for the unknown data, depending on how the datasets are selected.

Taken together, these results suggest that a model created by randomly selecting five datasets from 64 datasets and using them as a training dataset may have significantly poor prediction accuracy for the unknown data. This means that for the problem of predicting the radiation dose rates in a space containing a square pillar, which is the subject of this study, it is clear that five datasets are insufficient to create an accurate and stable model.

To improve model stability and generalization performance, it is necessary to increase the number of training datasets. Therefore, the mean R^2 values and SDs for the validation and the unknown data obtained from 100 Monte Carlo validation trials are shown in Figure 8, when 10, 15, ..., and 30 datasets are randomly selected from the total of 64 datasets. The mean, SD, maximum, and minimum R^2 values are summarized in Table 3. These results confirm that the mean R^2 values for the validation data are high and the SDs are low for all training datasets. The minimum R^2 value for the validation data is greater than 0.6290, indicating that the model is highly accurate. On the other hand, for the unknown data, the mean R^2 values are higher than

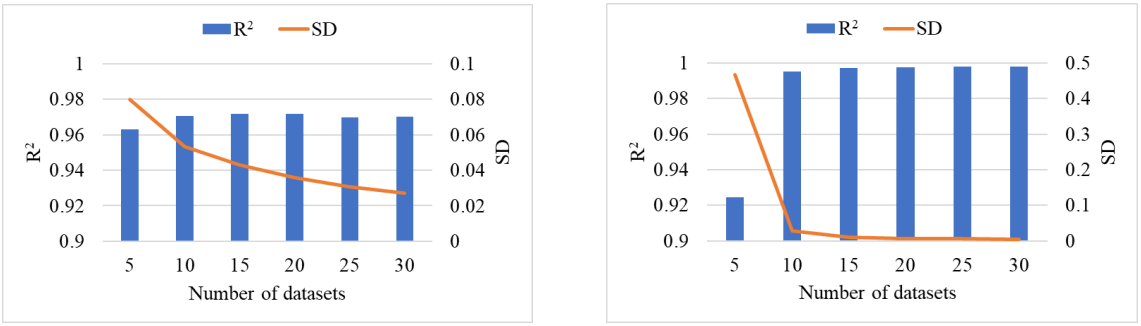

Figure 8: Mean R^2 values and SDs for both the validation data (left) and the unknown data (right), derived from 100 Monte Carlo cross-validation trails across various numbers of randomly selected training datasets.

Table 3: Mean, SD, maximum, and minimum R^2 values for both the validation data and the unknown data, based on 100 Monte Carloc cross-validation trails.

Number of trails	Validation data				Unknown data			
	Mean	SD	Max.	Min.	Mean	SD	Max.	Min.
5	0.9628	0.0798	0.9980	0.6290	0.9245	0.4661	0.9997	-18.59
10	0.9706	0.0533	0.9985	0.7653	0.9952	0.0271	0.9998	-2.910
15	0.9715	0.0431	0.9987	0.8570	0.9971	0.0096	0.9998	0.0453
20	0.9715	0.0357	0.9990	0.8792	0.9977	0.0062	0.9999	0.4764
25	0.9697	0.0308	0.9991	0.8933	0.9979	0.0054	0.9998	0.4782
30	0.9699	0.0270	0.9992	0.9187	0.9981	0.0047	0.9999	0.6676

0.92 for all training datasets. However, considering the SD, it is desirable to have more than 10 datasets. Furthermore, when considering the minimum value, the number of datasets should be 20 or more, and if possible, 30 or more is preferable. It is clear that the model can be constructed with generally good stability and generalization performance.

4 PREDICTION OF RADIATION DOSE RATE USING A SURROGATE MODEL

In this chapter, we use the surrogate model developed in the previous chapter to predict radiation dose rates in a space containing one or more square pillars. This model, constructed from 20 randomly selected training datasets, shows high accuracy, as evidenced by the R^2 values: 0.9975 for the training data and 0.9980 for the validation data.

4.1 The case of a space containing one square pillar

This section describes the distribution of radiation dose rates in a space containing one square pillar, using data randomly selected from the unknown data.

In the case of a single radiation source: Figure 9 displays isosurfaces derived from the surrogate model predictions and simulation results for radiation dose rates in a space. This space, selected randomly from the unknown data, includes a square pillar and a single radiation source located at positions 42 and 15, respectively. The figure demonstrates that the surrogate model's predictions closely match the simulation results. The R^2 for these predictions relative to the simulation results is 0.9994, indicating high prediction accuracy of the surrogate model.

In the case of multiple radiation sources: Utilizing the principle of superposition, the radiation dose rate distribution for the entire space is calculated by summing the dose rates from each radiation source. Figure 10 displays isosurfaces derived from the surrogate model predictions and the simulation results for a space containing a randomly selected pillar located at position 42 and five radiation sources located at positions 15, 4, 36, 32, and 29. The figure indicates that the surrogate model's predictions generally align with the simulation results. The R^2 for the surrogate model predictions relative to the simulation results is 0.7993, close to 0.8, indicating generally good prediction accuracy of the surrogate model.

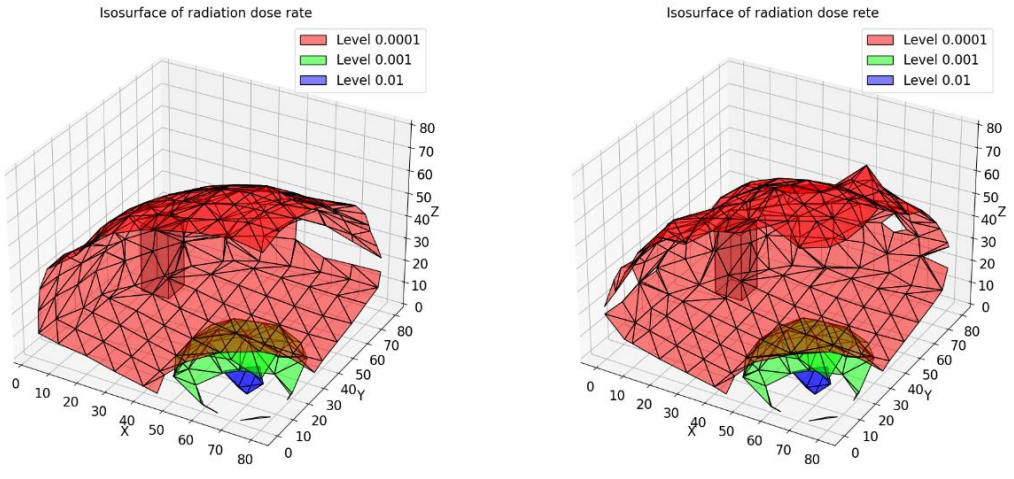

Surrogate Model Prediction Results Simulation results

Figure 9: Isosurfaces of radiation dose rate in a space with a square pillar and a radiation source. The R^2 for the surrogate model predictions is 0.9994.

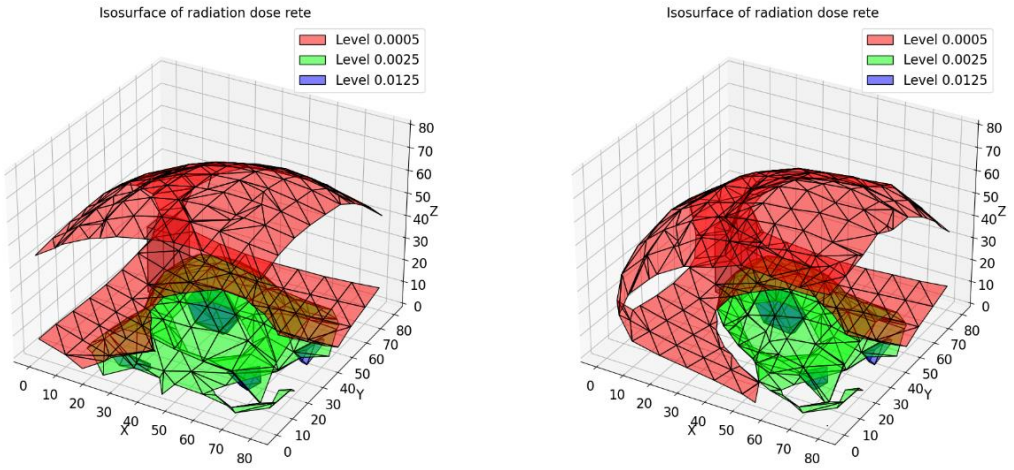

Surrogate Model Prediction Results Simulation results

Figure 9: Isosurfaces of radiation dose rate in a space with a square pillar and multiple radiation sources. The R^2 for the surrogate model predictions is 0.7993.

4.2 The case of a space containing multiple pillars

This section describes the distribution of radiation dose rates in a space containing multiple square pillars, randomly selected from the unknown data.

In the case of a single radiation source: The radiation dose rates in a space with multiple pillars and a single radiation source can be determined based on the principle of superposition. This involves summing the radiation dose rates obtained for each of the multiple pillars and dividing the results by the number of pillars. Figure 10 shows the isosurfaces based on the surrogate model predictions and the simulation results for the radiation dose rates in a space with five randomly selected pillars located at positions 42, 26, 62, 47, and 32, and a randomly selected radiation source located at position 19. The figure confirms that the surrogate model's predictions closely match the simulation results. The R^2 for the surrogate model's predictions relative to the simulation results is 0.9993, indicating very high prediction accuracy.

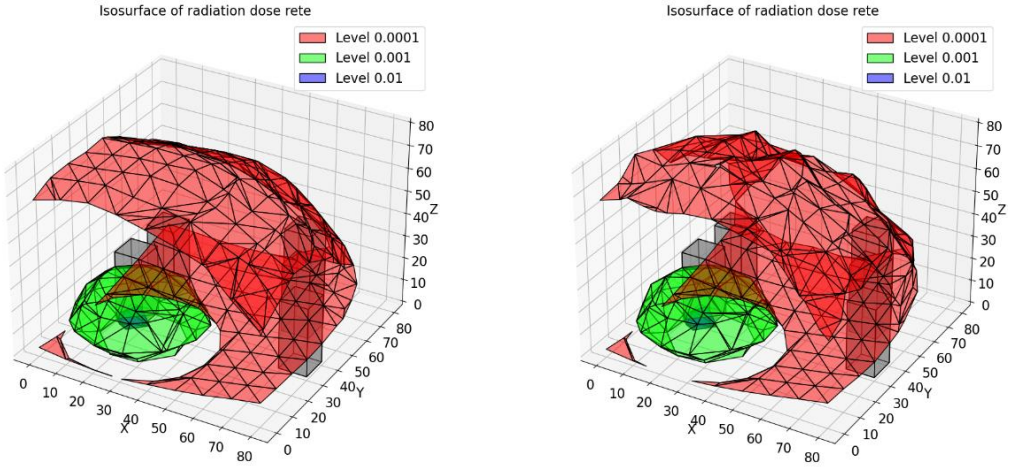

Surrogate Model Prediction Results Simulation results

Figure 10: Isosurfaces of radiation dose rate in a space with multiple square pillars and a radiation source. The R^2 for the surrogate model predictions is 0.9993.

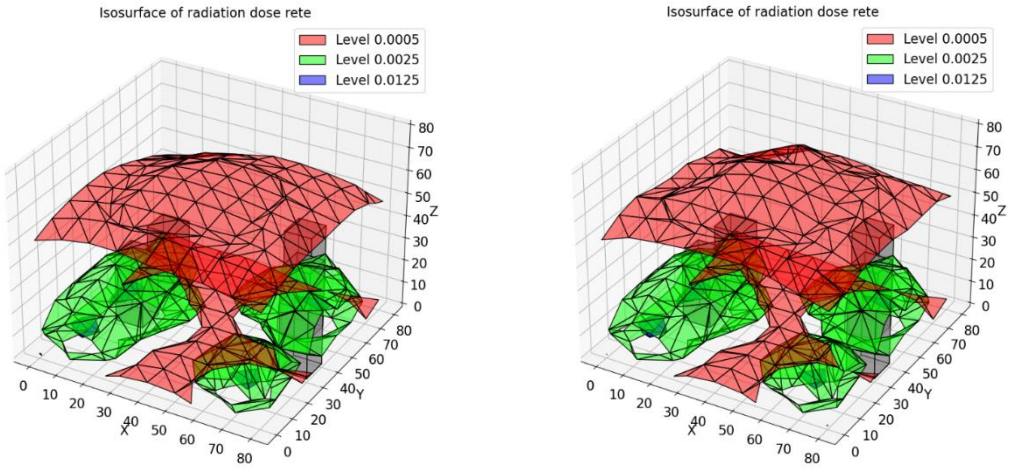

Surrogate Model Prediction Results Simulation results

Figure 11: Iso-surfaces of radiation dose rate in a space with multiple square pillars and multiple radiation sources, the R^2 for the surrogate model prediction results is 0.9900.

In the case of multiple radiation sources: Based on the principle of superposition, the radiation dose rates for a space with multiple pillars and multiple radiation sources can be obtained by summing the radiation dose rates for a space with one pillar and multiple radiation sources, as described in the previous section, and dividing the result by the number of pillars. Figure 11 shows the isosurfaces derived from the surrogate model predictions and the simulation results for the radiation dose rates in a space with five randomly selected pillars (42, 26, 62, 47, and 32) and five randomly selected radiation sources (15, 26, 74, 46, and 10). The figure indicates that the surrogate model's predictions are in good agreement with the simulation results. The R^2 for the surrogate model's predictions relative to the simulation results is 0.9900, which is very close to 1, indicating that the surrogate model has high prediction accuracy.

The discussion revealed that radiation dose rates in spaces with multiple pillars and sources can be obtained in real time using a surrogate model. Similarly, in reactor buildings with complex structures, radiation dose rates are determined by dividing the structures and sources into multiple parts. The surrogate model calculates the dose rate distribution for each part, and the overall distribution is derived by summing these results using the principle of superposition.

5 CONCLUSIONS

In this study, it was confirmed that the surrogate model, which can accurately predict the distribution of radiation dose rate in real time using deep learning as an alternative to simulation for a space containing a square pillar and a radiation source, shows good accuracy, stability, and generalization performance not only for the validation data but also for the unknown data. Based on the principle of superposition, the radiation dose rates in a space containing multiple pillars and radiation sources can be obtained by summing the results generated by the surrogate model for each pillar and source. Taken together, the following findings can be summarized:

- The coordinates indicating the location of the pillar and the radiation source, as well as the unit normal indicating the direction of the plane on which the radiation source resides, must be included in the training datasets as explanatory variables.
- For a space containing a pillar and a source, about 20 to 30 datasets are required to

create a surrogate model with good accuracy, stability, and generalization performance.
- Based on the principle of superposition, the distribution of the radiation dose rates in a space with multiple pillars and radiation sources can be obtained by summing the results obtained by the surrogate model for each pillar and radiation source.
- The above method of constructing a surrogate model to predict radiation dose rates in a space containing square pillars, combined with the principle of superposition, can be applied to the construction and application of a surrogate model to predict radiation dose rates in a nuclear reactor building containing complex structures.
- The surrogate model construction method used in this study can be applied to datasets consisting of grid points in space and corresponding physical quantities. For example, it could be used to create a surrogate model to predict the airflow in a space.

Acknowledgments: This study was conducted as part of the "Study on surrogation models for source and dose estimation analysis" (No. R05I119) commissioned by the Japan Atomic Energy Agency. The radiation dose rate simulation results used in this study were provided by Cybernet Systems, Inc. We express our deepest gratitude to them.

REFERENCES

[1] https://www.tepco.co.jp/decommission/progress/, (accessed on June 7, 2024) (in Japanese).
[2] https://1f-edu.mhlw.go.jp/contents/sc/pdf/03-00-00.pdf, (accessed on June 7, 2024) (in Japanese).
[3] Sato, T. et al., Recent improvements of the Particle and Heavy Ion Transport Code System - PHITS version 3.33. *J. Nucl. Sci. Technol.* (2024), **61**:127-135.
[4] Iwamoto, Y. et al., Benchmark Study of Particle and Heavy-ion Transport Code System Using Shielding Integral Benchmark Archive and Database for Accelerator-shielding Experiments. *J. Nucl. Sci. Technol.* (2022), **59**:665-675.
[5] Jiang, P., Zhou, Q. and Shao X. *Surrogate Model-Based Engineering Design and Optimization.* Springer (2020).
[6] Akasaka, K., Chen, F. and Teraguchi, T. Surrogate model development for prediction of car aerodynamics using machine learning. *Trans. Soc. Auto. Eng. Jpn.* (2021), **52**:621-626 (in Japanese).
[7] Liu, J., Kawata, A., Tanaka, M. and Akagi, T. Surrogate Models for Strength Prediction of Air Conditioning Compressor Parts Using machine learning. *Proceed. 34th Comput. Mech. Conf. Jpn. Soc. Mech. Eng.* (2021), F02_004 (in Japanese).
[8] Irikiin, M. and Iwata, Y. Basic study of temperature prediction method using CNN-based surrogate model and superposition principle. *Proceed. Conf. Comput. Eng. Sci.* (2023), A-10-03 (in Japanese).
[9] Shimokawa, T. et al. Construction of thermal boundary surrogate model using multiple regression analysis and deep learning for prediction of coolant temperature. *Trans. Soc. Auto. Eng. Jpn.* (2023), **54**:764-769 (in Japanese).
[10] Eda, Y. and Liu, J. Study of efficient sampling method for training data in building CAE surrogate model. *Proceed. 35th Comput. Mech. Conf. Jpn. Soc. Mech. Eng.* (2023), 3-03 (in Japanese).
[11] Mineta, R. et al. Efficiency of fast approximation analysis by simulation and machine learning using active learning. *Proceed. 2021 Manuf. Syst. Div. Conf. Jpn. Soc. Mech. Eng.* (2021), 79-80 (in Japanese).
[12] Stacey, W. M. *Nuclear Reactor Physics* (Third, Revised Edition). Wiley-VCH (2018).
[13] https://www.jaea.go.jp/02/press2018/p18111603/, (accessed on June 7, 2024) (in Japanese).
[14] https://phits.jaea.go.jp/rireki-manualj.html, (accessed on June 7, 2024) (in Japanese).